(data from three selected lines), consistent with stable differentiation. Furthermore, we confirmed rod induction by labeling with lentiviral vectors driving GFP from the Rhodopsin and Nrl promoters, either of which is specifically expressed in rod photoreceptors (**Fig. 2L–M**). Whole-cell patch-clamp recording demonstrated that the rod photoreceptor cell membrane contains voltage-dependent channels, suggesting that differentiated patient-derived rod cells are electrophysiologically functional (**Fig. 2N–O**). Meanwhile, the excluded iPS cell lines (ones that showed spontaneous differentiation during maintenance, or had a high copy number of transgenes), demonstrated a significant diversity of differentiation (**Fig. S7**). Together, these data show that patient-derived iPS cells can differentiate into cells that exhibit many of the immunochemical and electrophysiological features of mature rod photoreceptor cells.

Patient-specific rod cells undergo degeneration *in vitro*

As compared with normal iPS cells, there is no significant difference in rod cell differentiation efficiency at day 120 in K21(RP1)-, P101(PRPH2)-, and P59(RHO)-iPS cell lines (**Fig. 3**). iPS cells from both K11(RP9) and K10(RP9) carried a RP9 mutation; however, rod cell number was significantly lower than in normal iPS cells (**Fig. 3**). We asked whether early death of precursor cells leads to a smaller number of mature rod photoreceptor cells. To determine whether genetic mutations induce degeneration in photoreceptors cells *in vitro*, we extended the culture period and evaluated the number of rod photoreceptors at day 150. In differentiated iPS cells from patient K21(RP1) at day 150, the number of Rhodposin+ cells was significantly decreased (**Fig. 3**). For the K11-iPS cells, no Rhodposin+ cells were found at day 150 (**Fig. 3**). Importantly, some K11-cells at day 150 were positive for Recoverin (10.3±1.99%) and Crx, markers for the rod, cone photoreceptors, and/or bipolar cells (**Fig. 2K** and data not shown), strongly suggesting that cone photoreceptor and/or bipolar cells survived, whereas the rod photoreceptors underwent degeneration *in vitro*. In addition, we detected cells positive for Islet1 (a marker for retinal amacrine, bipolar and ganglion cells), again consistent with the survival of other types of retinal cells (**Fig. S6F**). From these results, we concluded that mature rod photoreceptors differentiated from patient iPS cells selectively degenerate in an RP-specific manner *in vitro*.

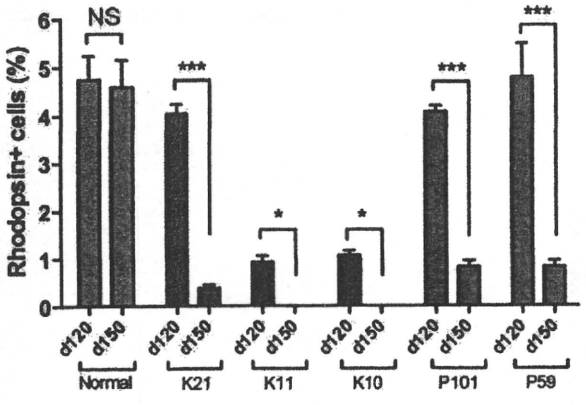

Figure 3. RP patient-derived rod photoreceptors undergo degeneration *in vitro*. iPS cells were differentiated into Rhodopsin+ rod photoreceptors in serum-free culture of embryoid body-like aggregates (SFEB culture). The percentages of Rhodopsin+ rod photoreceptors were evaluated at both day 120 and day 150, respectively. Data were from three independent iPS cell lines derived from the patients. ANOVA followed by Dunnett's test. * $p<0.05$; *** $p<0.001$. Values in the graphs are means and s.e.m.
doi:10.1371/journal.pone.0017084.g003

Cellular stresses involved in patient-derived rod cells

We next asked how the patient-derived rod photoreceptors degenerate. We evaluated apoptosis and cellular stresses in each cell line at both day 100 and day 120, respectively. Interestingly, in the RP9-iPS (K10 and K11) cells, a subset of Recoverin+ cells co-expressed cytoplasmic 8-hydroxy-2'-deoxyguanosine (8-OHdG), a major oxidative stress marker, indicating the presence of DNA oxidation in RP9 patient-derived photoreceptors by differentiation day 100 (**Fig. 4A** and **Fig. S8**). More caspase-3+ cells were presented in the Crx+ photoreceptor cluster of RP9-iPS than in those from other lines (**Fig. 4C–D**). After maturation of the rod photoreceptors from RP9-iPS cells, Rhodopsin+ cells co-expressed Acrolein, a marker of lipid oxidation (**Fig. 4E**), while no Rhodopsin+/Acrolein+ cells were observed in iPS cells derived from other patients carrying different mutations or in normal iPS cells (**Fig. 4F**). This pattern was similar to the cases of 8-OHdG and activated caspase-3. Thus, we conclude that oxidation is involved in the RP9-rod photoreceptor degeneration.

In differentiated RHO-iPS (P59) cells, we found that Rhodopsin proteins were localized in the cytoplasm (**Fig. 4G**), as determined by immunostaining with anti-Rhodopsin antibody (Ret-P1). This pattern is unlike the normal localization of Rhodopsin at the cell membrane in photoreceptors derived from normal iPS or other patient-derived iPS cells (**Fig. 4H** and data not shown). This result suggests accumulation of unfolded Rhodopsin, as reported previously in rhodopsin mutant mice cells [13]. We next examined the possible involvement of endoplasmic reticulum (ER) stress in RHO-iPS cell line degeneration. The Rhodopsin+ or Recoverin+ cells co-expressed immunoglobulin heavy-chain binding protein (BiP) or C/EBP homologous protein (CHOP), two conventional markers of endoplasmic reticulum (ER) stress, from day 120 (**Fig. 4I,K and Fig. S9**), while cells derived from control iPS or other mutant iPS cells were negative for BiP and CHOP (**Fig. 4J,L**). Taken together, these results demonstrate that ER stress is involved in rod photoreceptors carrying a RHO mutation.

Drug evaluation in patient-specific rod cells

The antioxidant vitamins α-tocopherol, ascorbic acid, and β-carotene have been tested in clinical trials as dietary therapies for RP [2] and in another major retinal degenerative disease, age-related macular degeneration [14]. Thus far, mostly due to the lack of appropriate validation models, there has been no evidence supporting the beneficial effects of these compounds on rod photoreceptors. We therefore assessed the effects of these agents on rod photoreceptors derived from patient iPS cells. In mouse retinal culture, short-term treatment with α-tocopherol, ascorbic acid and β-carotene at 100 μM, 200 μM and 1.6 μM, respectively, exerted no significant toxic effects on rod photoreceptor cells (**Fig. S10**). Since the differentiated rod photoreceptors underwent degeneration after day 120, we treated the cells for 7 days with these agents starting at day 120 (**Fig. 2A**). α-Tocopherol treatment significantly increased the number of Rhodopsin+ cells in iPS cells derived from K11- and K10-iPS with the RP9 mutation, while it had no significant effects on iPS cells with the either the RP1, PRPH2 or RHO mutation (**Fig. 5**). In contrast, neither ascorbic acid nor β-carotene treatment had any effect on iPS cells of any genotype (**Fig. S11**). We cannot currently explain the discrepancy between the effects of these antioxidants. It has been reported that under certain circumstances, anti-oxidants can act as "pro-oxidants" [15]. Taken together, our results indicate that treatment with α-tocopherol is beneficial to RP9-rod photoreceptor survival, and causes different effects on Rhodposin+ cells derived from different patients.

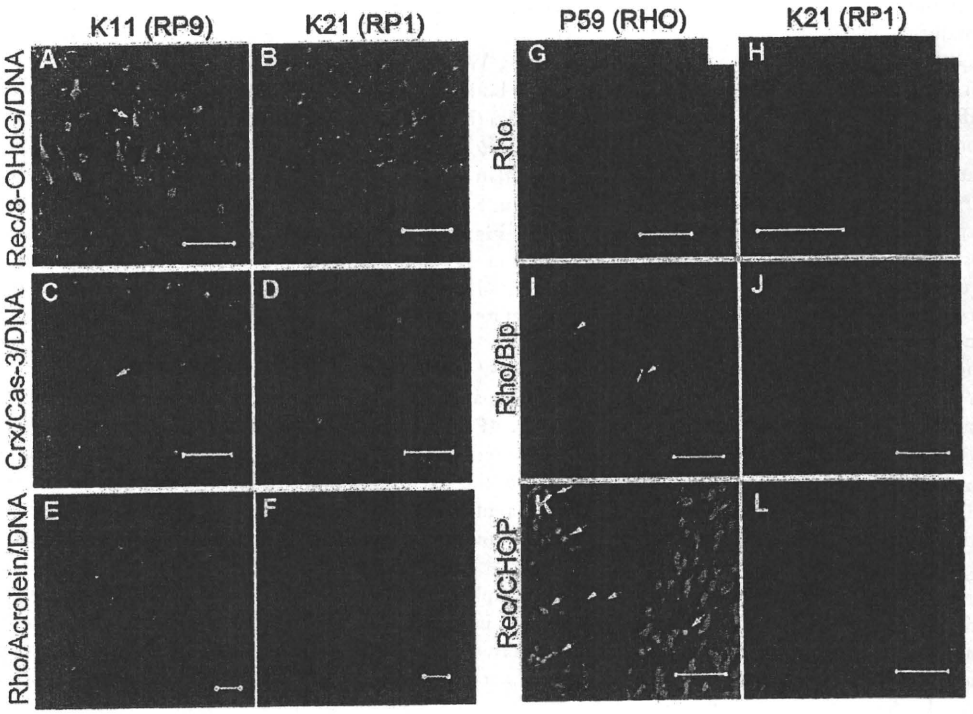

Figure 4. Cellular stress in patient-derived rod photoreceptor cells. Oxidative stress and apoptosis in differentiated rod photoreceptor cells derived from RP9-iPS (**A,C,E**) and RP1-iPS (**B,D,F**). (**A**) 8-OHdG, a marker for DNA oxidation, was found in K11- or K10-iPS–derived differentiated cells (day 100), but not in K21-iPS (**B**). Arrow indicates a cell double-positive for 8-OHdG and Recoverin. (**C**) The number of activated Caspase-3+ cells was greater in K11-iPS differentiation than in K21-iPS (**D**). From day 120, rod photoreceptor cells (Rhodopsin+) derived from RP9-iPS co-expressed the oxidative stress marker Acrolein (**E**); whereas RP1-iPS derivatives did not (**F**). (**G–L**) Abnormal cellular localization of Rhodopsin proteins and endoplasmic reticulum stress in RHO-iPS–derived rod photoreceptors. High magnification revealed cytoplasmic localization of Rhodopsin in rod photoreceptor cells carrying a RHO mutation (**G**) and a normal localization in the cell membrane in K21 cells (**H**). Rod cells derived from RHO-iPS co-expressed the ER stress markers BiP (**I**) and CHOP (**K**). K21-iPS–derived rod cells did not express BiP (**J**) or CHOP (**L**). Arrows indicate double-positive cells. Rec, Recoverin; Rho, Rhodopsin. All scale bars are 50 μm except for G and H (20 μm).
doi:10.1371/journal.pone.0017084.g004

Discussion

By using patient-derived iPS cells and *in vitro* differentiation technology, we have shown that RP9-retinitis pigmentosa is involved, at least in part, in oxidative stress pathways; this has not been reported previously in any animals or cell models. Furthermore, we have demonstrated that the antioxidant α-tocopherol exerts a beneficial effect on RP9-rod cells. Additionally, we have clearly shown that rod photoreceptors derived from patients with a RHO mutation are associated with ER stress; this is

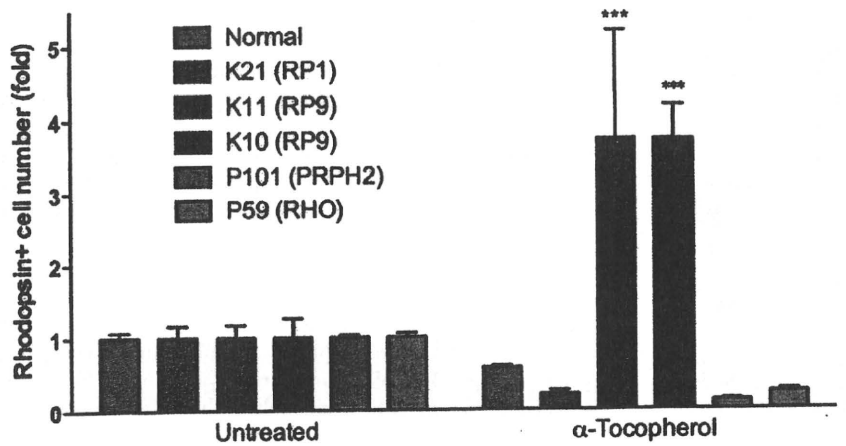

Figure 5. Disease modeling of patient-derived rod photoreceptor cells. α-Tocopherol treatment of patient-specific rod photoreceptors yielded a significant beneficial effect in RP9 mutant cells. Two-way ANOVA Bonferroni post-test showed no significance in other group (n = 3–8). Data represent 1–2 selected iPS cell lines of each patient. ***$p<0.001$. Values in the graphs are means and s.e.m.
doi:10.1371/journal.pone.0017084.g005

the first report of ER stress in a cell culture model for human rod cells. These cell models will be very useful for disease mechanism dissection and drug discovery. By screening several drugs that had already been tested in RP patients, we have revealed that rod photoreceptor cells derived from RP patients with different genetic subtypes exhibit significant differences in drug responses. Among the different types of antioxidants, α-tocopherol has either beneficial or non-beneficial effects on diseased photoreceptors, depending on the genetic mutation. This is the first report of the utilization of iPS cells related to personalized medicine, which will be helpful for routin clinical practice. Our results also provided evidence that genetic diagnosis is essential for optimizing personalized treatment for patients with retinal degenerative diseases [11]. An important future study made possible by this work is the screening of a compound library for drugs that could be used to treat RP. Patient-derived iPS cells revealed differences in pathogenesis and the efficacy of antioxidants among patients with different disease-causing mutations. Although the microenvironment affects the pathogenesis of diseases, and *in vitro* evaluation is not perfect, this study suggests that iPS cells could be used to select between multiple available treatments, allowing physicians to advise each patient individually. The weakness of our method for disease modeling is that differentiation requires a long period of time. Shortening the induction period and identifying appropriate surface markers for rod cells will improve disease modeling using patient-specific iPS cells.

In brief, we generated pluripotent stem cells from retinitis pigmentosa patients and induced them into retinal cells. Compared with normal cells, patient-derived rod cells simulated the disease phenotype and exhibited different responses to specific drugs. We found that patient-specific rod cells underwent degeneration *in vitro*, which maybe related to different cellular stresses. To our knowledge, this is the first report of disease modeling of retinal degeneration using patient-derived iPS cells.

Supporting Information

Figure S1 Pedigrees of K21 (A), P59 (B), K10 and K11 (C). Families of P59 (**B**) and K10 and K11 (**C**) show autosomal dominant mode of inheritance. (**C**) Mutation analysis was performed in four patients and two normal relatives in the RP9 family. The H137L mutation in RP9 gene was co-segregated with the disease in the family. Closed symbols indicate individuals with RP and open symbols indicate unaffected subjects. Question marks indicate symptom unknown. The bars above the symbols indicate examined subjects. Arrow, proband; slash, deceased.
(TIF)

Figure S2 Mutation in the *RP9* gene. (**A**) Alignment of RP9 sequence and pseudo-gene shows the same nucleotide in the mutated location. (**B**) Sequence chromatogram of cDNA sequence demonstrates the c.410A>T (H137L) mutation in the *RP9* gene, instead of the paralogous variant in pseudo-gene which was documented in RetNet (www.sph.uth.tmc.edu/retnet/disease.htm).
(JPG)

Figure S3 Selection by colony morphology. (**A**) iPS colony (K21S4) shows ES-like morphology. (**B**) Spontaneous differentiation in the colony during maintenance (K21S14). Scale bars, 50 μm.
(TIF)

Figure S4 Quantification of transgene copy number. Total copy number of four transgenes in the selected iPS lines. Selected iPS cells with fewest integrations and two high copy number lines used for *in vitro* differentiation.
(TIF)

Figure S5 Efficiency of RPE induction in patient-iPS cells. RPE production of the five patient-iPS cells showed no significant differences (n = 4). Data represent the percentage of RPE area at differentiation day 60. One-way ANOVA followed by Dunnett's test. Values are mean and s.e.m.
(TIF)

Figure S6 Induced retinal cells from patient iPS cells (K21S4). Crx+ photoreceptor precursor cells present in the cell cluster on differentiation day 60 (A). Crx+ cells co-expressed Recoverin, indicating differentiation into photoreceptor cells (B). Rhodopsin+ cells had a long process at day 150 (C). In the differentiated cells, we also observed cells positive of PKCα (a marker for bipolar cells) (D). Cells positive for Math5 and Brn3b (markers for ganglion progenitor or ganglion cells (day 60) (E). Cells positive for Islet-1 (a marker for amacrine, bipolar and ganglion cells) (F). Scale bars, 50 μm (A, D, E, and F); 20 μm (B and C).
(TIF)

Figure S7 Differentiation of the patient-iPS cells. iPS colony was cut into uniform sized pieces (**A**) and subjected to a floating culture (P59M8, day 20) (**B**). RPE (pigmented) and recoverin+ (green) cells were efficiently induced (P59M8, day 60) (**C**). (**D**) An excluded iPS line, P59M16, with high number transgenes showed a striking lentoid formation during the floating culture (day 20). Scale bars, 50 μm.
(TIF)

Figure S8 Oxidative stress in photoreceptor cells with the RP9 mutation (K11). (A) Recoverin, (B) 8-OHdG, (C) Recoverin/8-OHdG, (D) Recoverin/8-OHdG/DNA. Arrows indicate cells with weak Recoverin signal positive for 8-OHdG; Arrowheads represent cells with strong Recoverin signal positive for 8-OHdG; Asterisks represent Recoverin+ cells negative for 8-OHdG. Scale bar, 50 μm.
(JPG)

Figure S9 ER stress in photoreceptor cells with the RHO mutation (P59). (A) CHOP, (B) Recoverin, (C) Recoverin/CHOP, (D) Recoverin/CHOP/DNA. Arrows indicate cells with weak Recoverin signals positive for CHOP in nuclei; Arrowheads represent cells with strong Recoverin signals positive for CHOP; Asterisks represent Recoverin+ cells negative for CHOP. Scale bar, 50 μm.
(JPG)

Figure S10 Toxicity testing of the antioxidants in murine retina-derived rod photoreceptor cells. Primary culture of mouse retinal cells treated with 100 μM α-tocopherol, 200 μM ascorbic acid or 1.6 μM β-carotene for 24 hours and the rod photoreceptors were counted using flow cytometry. Value represents the ratio of treated-rod photoreceptors compared with control cells. n = 4. One-way ANOVA followed by Dunnett's test. Values are mean and s.e.m. NS, not significant.
(JPG)

Figure S11 Differentiated rod cells from normal and patient iPS cells treated with 200 μM ascorbic acid or 1.6 μM β-carotene did not show statistically significant differences. Two-way ANOVA Bonferroni post-test. Values are mean and s.e.m.
(JPG)

Table S1 Phenotypic data of the RP patients. M, male; F, female; AD, age at diagnosis; BCVA, best corrected visual acuity; HM, hand motion.
(DOC)

Table S2 Antibodies used in the present study.
(DOC)

Acknowledgments

We thank C. Ishigami and Y. Tada for assistance of mutation screening; K. Iseki, N. Sakai, Y. Wataoka, K. Sadamoto, A. Tachibana, C. Yamada for technical assistance; Y. Arata, W. Meng, C. Li, A. Suga, M. Mandai and all members in the Takahashi lab for advice.

Author Contributions

Conceived and designed the experiments: ZBJ MT. Performed the experiments: ZBJ SO FO KH JA. Analyzed the data: ZBJ SO FO. Contributed reagents/materials/analysis tools: MT YH TI. Wrote the paper: ZBJ MT.

References

1. Weleber RG, Gregory-Evans K (2006) Retinitis Pigmentosa and Allied Disorders. In: Hilton DR, Schachat AP, Ryan SJ, eds. Retina. Elsevier Mosby. pp 395–498.
2. Berson EL, Rosner B, Sandberg MA, Hayes KC, Nicholson BW, et al. (1993) A randomized trial of vitamin A and vitamin E supplementation for retinitis pigmentosa. Arch Ophthalmol 11: 761–772.
3. Takahashi K, Tanabe K, Ohnuki M, Narita M, Ichisaka T, et al. (2007) Induction of pluripotent stem cells from adult human fibroblasts by defined factors. Cell 131: 861–872.
4. Yu J, Vodyanik MA, Smuga-Otto K, Antosiewicz-Bourget J, Frane JL, et al. (2007) Induced pluripotent stem cell lines derived from human somatic cells. Science 318: 1917–1920.
5. Park IH, Arora N, Huo H, Maherali N, Ahfeldt T, et al. (2008) Disease-specific induced pluripotent stem cells. Cell 134: 877–886.
6. Raya A, Rodríguez-Pizà I, Guenechea G, Vassena R, Navarro S, et al. (2009) Disease-corrected haematopoietic progenitors from Fanconi anaemia induced pluripotent stem cells. Nature 460: 53–59.
7. Yamanaka S (2007) Strategies and new developments in the generation of patient-specific pluripotent stem cells. Cell Stem Cell 1: 39–49.
8. Osakada F, Ikeda H, Mandai M, Wataya T, Watanabe K, et al. (2008) Toward the generation of rod and cone photoreceptors from mouse, monkey and human embryonic stem cells. Nat Biotechnol 26: 215–224.
9. Osakada F, Jin ZB, Hirami Y, Ikeda H, Danjyo T, et al. (2009) In vitro differentiation of retinal cells from human pluripotent stem cells by small-molecule induction. J Cell Sci 122: 3169–3179.
10. Hirami Y, Osakada F, Takahashi K, Okita K, Yamanaka S, et al. (2009) Generation of retinal cells from mouse and human induced pluripotent stem cells. Neurosci Lett 458: 126–131.
11. Jin ZB, Mandai M, Yokota T, Higuchi K, Ohmori K, et al. (2008) Identifying pathogenic genetic background of simplex or multiplex retinitis pigmentosa patients: a large scale mutation screening study. J Med Genet 45: 465–472.
12. Ikeda H, Osakada F, Watanabe K, Mizuseki K, Haraguchi T, et al. (2005) Generation of Rx+/Pax6+ neural retinal precursors from embryonic stem cells. Proc Natl Acad Sci U S A 102: 11331–11336.
13. Sung CH, Davenport CM, Nathans J (1993) Rhodopsin mutations responsible for autosomal dominant retinitis pigmentosa. Clustering of functional classes along the polypeptide chain. J Biol Chem 268: 26645–26649.
14. van Leeuwen R, Boekhoorn S, Vingerling JR, Witteman JC, Klaver CC, et al. (2005) Dietary intake of antioxidants and risk of age-related macular degeneration. JAMA 294: 3101–3107.
15. van Helden YG, Keijer J, Heil SG, Picó C, Palou A, et al. (2009) Beta-carotene affects oxidative stress-related DNA damage in lung epithelial cells and in ferret lung. Carcinogenesis 30: 2070–2076.

Chapter 9
Suppression of Drusen Formation by Compstatin, a Peptide Inhibitor of Complement C3 activation, on Cynomolgus Monkey with Early-Onset Macular Degeneration

Zai-Long Chi, Tsunehiko Yoshida, John D. Lambris, and Takeshi Iwata

Abstract For the past 10 years, number of evidence has shown that activation of complement cascade has been associated with age-related macular degeneration (AMD). The genome wide association study in American population with dominantly dry-type AMD has revealed strong association with single nucleotide polymorphism (SNP) of complement genes. Protein composition of drusen, a deposit observed in sub-retinal space between Bruch's membrane and retinal pigment epithelial (RPE), contains active complement molecules in human and monkey. These evidences have leaded us to consider the possibility of suppressing complement cascade in the retina to delay or reverse the onset of AMD. To test is hypothesis we used the C3 inhibitor Compstatin on primate model with early-onset macular degeneration which develop drusen in less than 2 years after birth. Our preliminary result showed drusen disappearance after 6 months of intravitreal injection.

1 AMD and Association of Complement Related Genes

The most prevalent eye disease for elderly Europeans and Americans is AMD. AMD is a blinding disorder characterized by a marked decrease in central vision associated with retinal pigment epithelial (RPE) atrophy with or without choroidal neovascularization (CNV). The non-neovascular type is called the dry-type AMD and includes more than 80% of the cases, and the neovascular type is called the wet-type AMD which is progressive with a higher probability of blindness. In some cases of CNV, the new vessels penetrate Bruch's membrane and pass into the sub-retinal space. The progressive impairment of the RPE and damage to Bruch's membrane and choriocapillaris results in retinal atrophy and photoreceptor dysfunction.

Z.-L. Chi (✉)
Division of Molecular & Cellular Biology, National Institute of Sensory Organs, National Hospital Organization Tokyo Medical Center, Tokyo, Japan
e-mail: chizai-long@kankakuki.go.jp

J.D. Lambris and A.P. Adamis (eds.), *Inflammation and Retinal Disease: Complement Biology and Pathology*, Advances in Experimental Medicine and Biology 703,
DOI 10.1007/978-1-4419-5635-4_9, © Springer Science+Business Media, LLC 2010

Genetic, behavioral, and environmental factors are believed to be involved for the onset of this disease. The prevalence of AMD differs considerably among the different ethnic groups, but the incidence increases with age in all groups. Epidemiological studies have shown that genetic factor play critical role for AMD. However, only a small proportion of the families with AMD show Mendelian inheritance, and the majority of the individuals inherit AMD in a complex multi-gene pattern. With the help of the haplotype marker project (HapMap Project), genome wide scanning has identified at least 13 loci linked to AMD on different chromosomes (Iyengar et al. 2004; Schick et al. 2003; Majewski et al. 2003). Other risk factors such as cigarette smoking, obesity, hypertension, and atherosclerosis are also associated with the disease.

Recently, a polymorphism of complement factor H (CFH) gene (Y402H) was shown to be associated with an increased risk for AMD (Klein et al. 2005; Edwards et al. 2005; Haines et al. 2005; Hageman et al. 2005). These results were confirmed in many of the countries with large Caucasian populations but not in Japan (Okamoto et al. 2006; Gotoh et al. 2006). This gene is located on chromosome 1q25–31 where one of the candidate loci was identified by whole genome association studies by linkage markers. Another recent study reported that a haplotype association of tandemly located complement 2 and factor B (Gold et al. 2006) was protective and C3 (Yates et al. 2007) as risk for AMD. HTRA1, a serine protease 11 was recently discovered to be strongly associated with AMD (Yang et al. 2006; Dewan et al. 2006). Unlike the CFH, our study shows strongly association with this gene for Japanese AMD patients (Yoshida et al. 2007). This difference of gene association is probably related to the difference of AMD type dominant in each country. Our genome wide association study on Japanese population with typical wet-type AMD and polypoidal choroidal vasculopathy (PCV) shows significant association at p-value of 10^{-14} and 10^{-7} respectively for ARMS2/Htra1 locus. However when much lower associated SNPs of CFH or C3 or combined the odds ratio significantly increased (Goto et al. 2009)

2 Activated Complement Component in Drusen

The early stage of the dry-type AMD is characterized by thickening of Bruch's membrane, aggregation of pigment granules, and increasing numbers of drusen. Drusen are small yellowish-white deposits that are composed of lipids, proteins, glycoproteins, and glycosaminoglycans. They accumulate in the extracellular space and the inner aspects of Bruch's membrane. Drusen are not directly associated with visual loss but represent a risk factor for dry-type AMD. The classification of hard and soft drusen is based on their size, shape, and color; hard drusen are yellowish with diameters <50 μm and are found in eyes that are less likely to progress to advanced stages of the disease, while soft drusen are darker yellow and larger in size, and are found in eyes more likely to progress to more advanced stages of AMD.

Both immunohistochemistry and proteomic techniques have shown that drusen are composed of molecules that mediate inflammatory and immune processes (Russell et al. 2000; Mullins et al. 2000). These molecules include components of the complement pathway and modulators of complement activation, viz., vitronectin, clusterin, membrane cofactor protein, and complement receptor-1. In addition, molecules triggering inflammation, amyloid P component, α1-antitrypsin, and apolipoprotein E, were identified in drusen. Cellular debris from macrophages, RPE cells, and choroidal dendritic cells has been also identified in drusen. Additional proteins such as crystallins, EEFMP1, and amyloid-beta have been found in drusen. The presence of immunoreactive proteins and the oxidative modifications of many proteins in drusen imply that both oxidation and immune functions are involved in the pathogenesis of AMD. Finding of these molecules suggest that complement activation triggers innate immune responses in the subretinal space.

3 Cynomolgus Monkey with Early-Onset Macular Degeneration

Over the past years non-human primates with well-defined fovea has been the target for AMD research. A monkey with macular degeneration was first described by Stafford et al. in 1974. They reported that 6.6% of the elderly monkeys they examined showed pigmentary disorders and drusen-like spots (Stafford et al. 1984). We also observed at approximately the same rate of disorder in elderly cynomolgus monkeys in the Philippines primate facility (SICONBREC) (Umeda et al. 2005a, b). El-Mofty et al. (1978) reported that the incidence of maculopathy was 50% in a colony of rhesus monkeys at the Caribbean Primate Research Center of the University of Puerto Rico. In 1986, a single cynomolgus monkey (*Macaca fascicularis*) with large number of small drusen in the macula was found in Tsukuba Primate Research Center at Tsukuba City, Japan (Nicolas et al. 1996a, b; Suzuki et al. 2003). This single affected monkey has been bred to a large pedigree of more than 300 monkeys (Fig. 1). Drusen are observed in the macula as early as 2 years after birth, and the number increase and spread toward the peripheral retina throughout life (Figs. 2–3). Histological abnormalities of the retina and abnormal electroretinogram (ERG) were observed in sever case showing physiological dysfunction of the macula.

Immunohistochemical and proteomic analyses of the drusen from these monkeys showed that the drusen were very similar to those in other monkeys with aged macular degeneration sporadically found in older monkeys and also with human drusen (Umeda et al. 2005a, b; Ambati et al. 2003). These observations have shown that TPRC monkeys produce drusen that are biochemically similar to those in human AMD patients, but the development of the drusen occurs at an accelerated rate.

More than 240 loci are being investigated to try to identify the disease causing gene and to understand the biological pathways leading to complement activation. Simultaneously, we have been studying a colony of aged monkeys in SICONBREC,

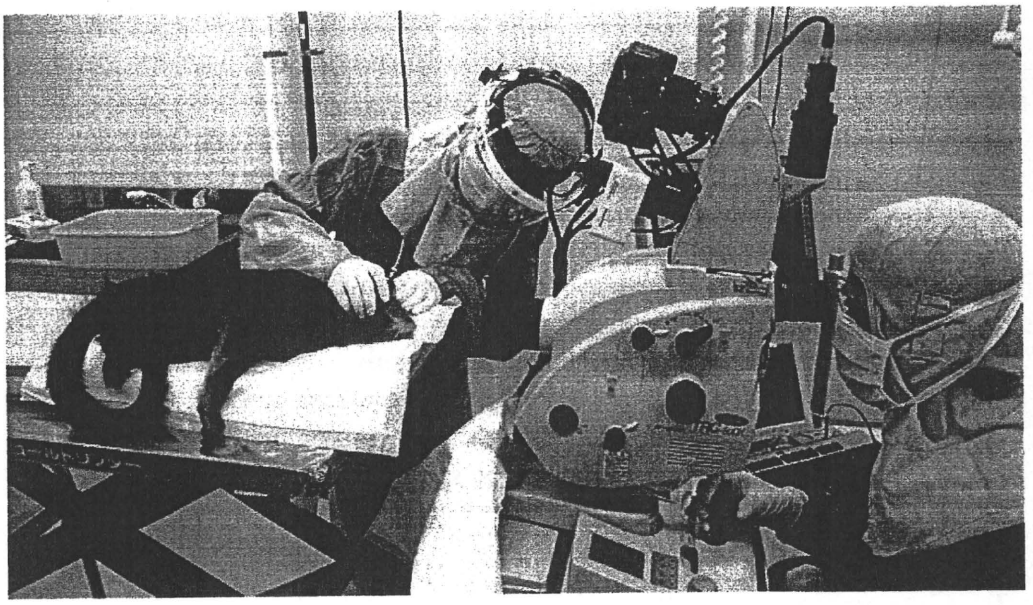

Fig. 1 Fundus photography of affected monkey at TPRC

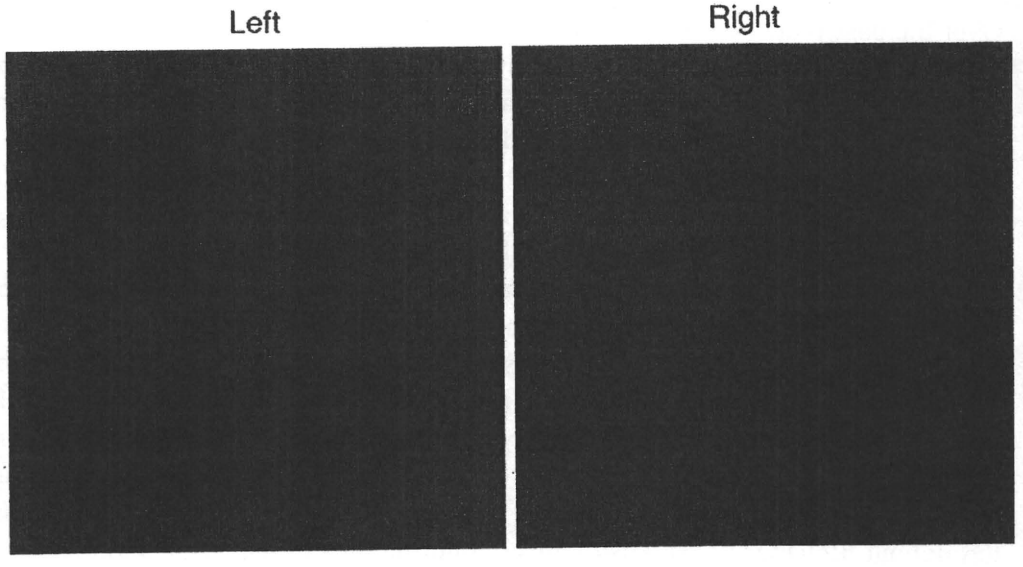

Fig. 2 Fundus photograph of affected monkey showing accumulation of drusen in macula of both eyes

which develop drusen after 15 years of birth. Drusen components of these sporadically found affected monkeys were compared with human and TPRC monkeys by immunohistochemistry and proteomic analysis using ion spray mass spectrometer. Significant finding was that drusen contained protein molecules that mediate inflammatory and immune processes. These include immunoglobulins, components of complement pathway, and modulators for complement activation (e.g., vitronectin, clusterin, membrane cofactor protein, and complement receptor-1), molecules involved in the acute-phase response to inflammation (e.g., amyloid P component,

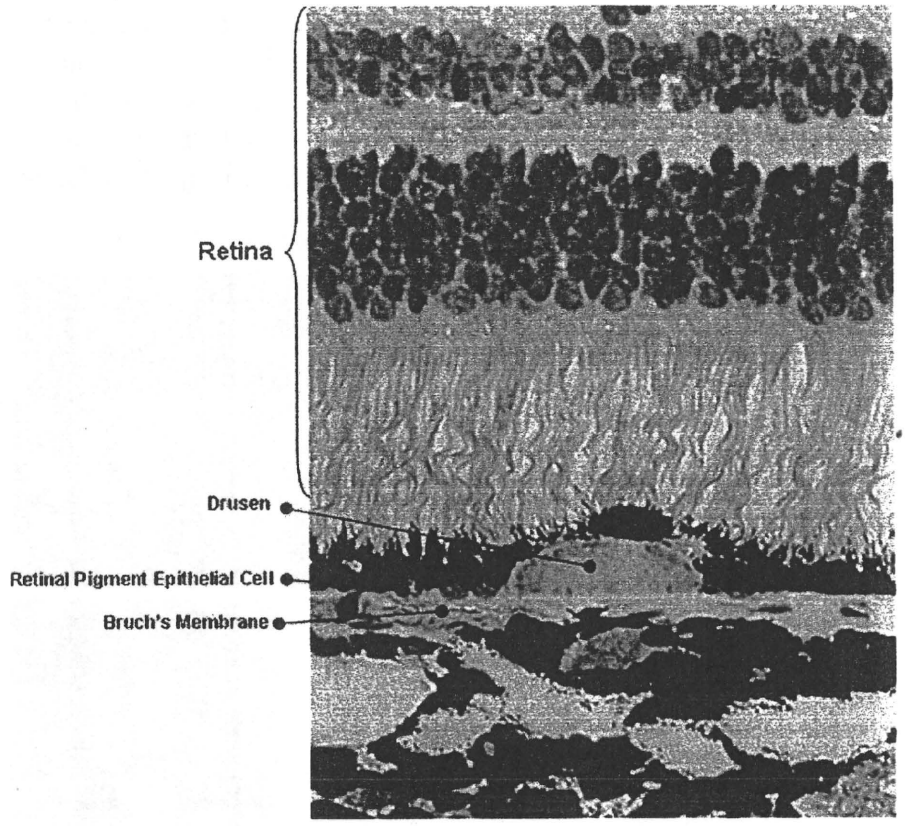

Fig. 3 Retinal histological section of affected monkey showing the accumulation of drusen

α1-antitrypsin, and apolipoprotein E), major histocompatibility complex class II antigens, and HLA-DR antigens (Umeda et al. 2005a, b). Cellular components have also been identified in drusen, including RPE debris, lipofuscin, and melanin, as well as processes of choroidal dendritic cells, which contribute to the inflammatory response. The presence of immunoreactive proteins and oxidative modified proteins implicate both oxidation and immune functions in the pathogenesis of affected monkeys.

4 Suppression and Reversal of Drusen Formation by Compstatin

To test the effect of long term suppression of complement activation in the retina, an cyclic analogue (Ac-I[CV(1MeW)QDWGAHRC]T-NH2) of the small cyclic synthetic peptide compstatin (Katragadda et al. 2006) was intravitreally injected into eight affected monkeys at different dose and intervals. Four affected monkeys were injected at 1 mg dose at 1 month interval while other four affected monkeys at 50 μg dose at 1 week interval. Both 1 mg or 50 μg dose were dissolved in 100 μl of saline solution, filtrated and intravitreally injected using 30G needle.

Due to the unique molecular characteristic of compstatin, immediately after injection, compstatin precipitate and form gel-like structure in the vitreous. This gel will gradually dissolve and disappear after 6 months. Four monkeys injected with 1 mg for 3 months developed significant opacity to the point where fundus observation was impossible. These monkeys were halted for further injection. On the other

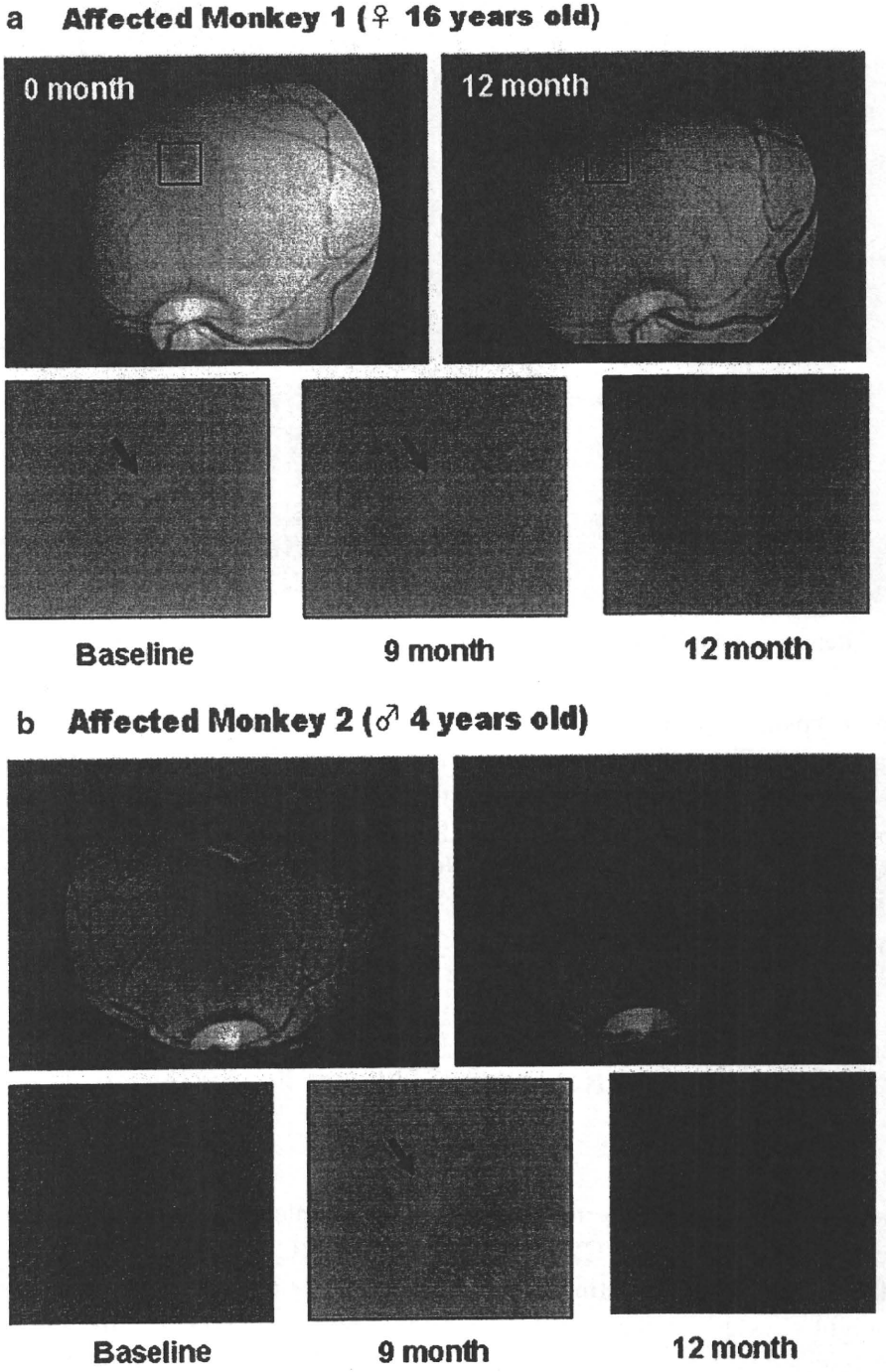

Fig. 4 Suppression and reversal of drusen formation after 9 months of intravitreal injection of 50 μl compstatin at 1 week interval

hand, vitreous of four monkeys with 50 μg dose were clear within 2 days. After 6 months of injection, we noticed diffusion of drusen in the macula and by 9 months partial disappearance of drusen was observed in all four monkeys (Fig. 4). This preliminary experiment has shown reversal of drusen formation by suppression of complement activation. To explain this reversal phenomenon, which has not been observed in untreated affected monkeys, will require further experiments including identification of disease causing gene and pathway leading to complement activation. The information should benefit for development of improved drug and therapy for future AMD prevention.

All experimental procedures for this primate study were approved by the Animal Welfare and Animal Care Committee of the TRPC and the Experimental Animal Committee of the National Tokyo Medical Center. The facilities are accredited by the Association for Assessment and Accreditation of Laboratory Animal Care International (AAALAC International). Monkeys were routinely examined for physical and ophthalmic conditions by veterinarians and by ophthalmologists, respectively.

Acknowledgements This work was supported by the research grants from the Japanese Ministry of Health, Labour and Welfare (TI) and NIH grants GM-62134, and AI-068730 (JDL). The authors thank Cedric Francois and Paul Olson of Potentia Pharmaceuticals Inc., for providing us the GM grade compstatin.

References

Ambati J, Anand A, Fernandez S, Sakurai E, Lynn BC, Kuziel WA, Rollins BJ, Ambati BK (2003) An animal model of age-related macular degeneration in senescent Ccl-2- or Ccr-2-deficient mice. Nat Med 9:1390–1397

Dewan A, Liu M, Hartman S, Zhang SS, Liu DT, Zhao C, Tam PO, Chan WM, Lam DS, Snyder M, Barnstable C, Pang CP, Hoh J (2006) HTRA1 promoter polymorphism in wet age-related macular degeneration. Science 314:989–992

Edwards AO, Ritter R 3rd, Abel KJ, Manning A, Panhuysen C, Farrer LA (2005) Complement factor H polymorphism and age-related macular degeneration. Science 308:421–424

El-Mofty A, Gouras P, Eisner G, Balazs EA (1978) Macular degeneration in rhesus monkey (*Macaca mulatta*). Exp Eye Res 27:499–502

Gold B, Merriam JE, Zernant J, Hancox LS, Taiber AJ, Gehrs K, Cramer K, Neel J, Bergeron J, Barile GR, Smith RT, AMD Genetics Clinical Study Group, Hageman GS, Dean M, Allikmets R (2006) Variation in factor B (BF) and complement component 2 (C2) genes is associated with age-related macular degeneration. Nat Genet 38:458–462

Goto A, Akahori M, Okamoto H, Minami M, Terauchi N, Haruhata Y, Obazawa M, Noda T, Honda M, Mizota A, Tanaka M, Hayashi T, Tanito M, Ogata N, Iwata T (2009) Genetic analysis of typical wet-type age-related macular degeneration and polypoidal choroidal vasculopathy in Japanese population. J Biochem Dis Inform 2(4):164–175

Gotoh N, Yamada R, Hiratani H, Renault V, Kuroiwa S, Monet M, Toyoda S, Chida S, Mandai M, Otani A, Yoshimura N, Matsuda F (2006) No association between complement factor H gene polymorphism and exudative age-related macular degeneration in Japanese. Hum Genet 120:139–143

Hageman GS, Anderson DH, Johnson LV, Hancox LS, Taiber AJ, Hardisty LI, Hageman JL, Stockman HA, Borchardt JD, Gehrs KM, Smith RJ, Silvestri G, Russell SR, Klaver CC,

Barbazetto I, Chang S, Yannuzzi LA, Barile GR, Merriam JC, Smith RT, Olsh AK, Bergeron J, Zernant J, Merriam JE, Gold B, Dean M, Allikmets R (2005) A common haplotype in the complement regulatory gene factor H (HF1/CFH) predisposes individuals to age-related macular degeneration. Proc Natl Acad Sci USA 102:7227–7232

Haines JL, Hauser MA, Schmidt S, Scott WK, Olson LM, Gallins P, Spencer KL, Kwan SY, Noureddine M, Gilbert JR, Schnetz-Boutaud N, Agarwal A, Postel EA, Pericak-Vance MA (2005) Complement factor H variant increases the risk of age-related macular degeneration. Science 308:419–421

Iyengar SK, Song D, Klein BE, Klein R, Schick JH, Humphrey J, Millard C, Liptak R, Russo K, Jun G, Lee KE, Fijal B, Elston RC (2004) Dissection of genomewide-scan data in extended families reveals a major locus and oligogenic susceptibility for age-related macular degeneration. Am J Hum Genet 74:20–39

Katragadda M, Magotti P, Sfyroera G, Lambris JD (2006) Hydrophobic effect and hydrogen bonds account for the improved activity of a complement inhibitor, compstatin. J Med Chem 49:4616–4622

Klein RJ, Zeiss C, Chew EY, Tsai JY, Sackler RS, Haynes C, Henning AK, SanGiovanni JP, Mane SM, Mayne ST, Bracken MB, Ferris FL, Ott J, Barnstable C, Hoh J (2005) Complement factor H polymorphism in age-related macular degeneration. Science 308:385–389

Majewski J, Schultz DW, Weleber RG, Schain MB, Edwards AO, Matise TC, Acott TS, Ott J, Klein ML (2003) Age-related macular degeneration – a genome scan in extended families. Am J Hum Genet 73:540–550

Mullins RF, Russell SR, Anderson DH, Hageman GS (2000) Drusen associated with aging and age-related macular degeneration contain proteins common to extracellular deposits associated with atherosclerosis, elastosis, amyloidosis, and dense deposit disease. FASEB J 14:835–846

Nicolas MG, Fujiki K, Murayama K, Suzuki MT, Mineki R, Hayakawa M, Yoshikawa Y, Cho F, Kanai A (1996a) Studies on the mechanism of early onset macular degeneration in cynomolgus (*Macaca fascicularis*) monkeys. I. Abnormal concentrations of two proteins in the retina. Exp Eye Res 62:211–219

Nicolas MG, Fujiki K, Murayama K, Suzuki MT, Shindo N, Hotta Y, Iwata F, Fujimura T, Yoshikawa Y, Cho F, Kanai A (1996b) Studies on the mechanism of early onset macular degeneration in cynomolgus monkeys. II. Suppression of metallothionein synthesis in the retina in oxidative stress. Exp Eye Res 62:399–408

Okamoto H, Umeda S, Obazawa M, Minami M, Noda T, Mizota A, Honda M, Tanaka M, Koyama R, Takagi I, Sakamoto Y, Saito Y, Miyake Y, Iwata T (2006) Complement factor H polymorphisms in Japanese population with age-related macular degeneration. Mol Vis 12:156–158

Russell SR, Mullins RF, Schneider BL, Hageman GS (2000) Location, substructure, and composition of basal laminar drusen compared with drusen associated with aging and age-related macular degeneration. Am J Ophthalmol 129:205–214

Schick JH, Iyengar SK, Klein BE, Klein R, Reading K, Liptak R, Millard C, Lee KE, Tomany SC, Moore EL, Fijal BA, Elston RC (2003) A whole-genome screen of a quantitative trait of age-related maculopathy in sibships from the Beaver Dam Eye Study. Am J Hum Genet 72:1412–1424

Stafford TJ, Anness SH, Fine BS (1984) Spontaneous degenerative maculopathy in the monkey. Ophthalmology 91:513–521

Suzuki MT, Terao K, Yoshikawa Y (2003) Familial early onset macular degeneration in cynomolgus monkeys (*Macaca fascicularis*). Primates 44:291–294

Umeda S, Ayyagari R, Allikmets R, Suzuki MT, Karoukis AJ, Ambasudhan R, Zernant J, Okamoto H, Ono F, Terao K, Mizota A, Yoshikawa Y, Tanaka Y, Iwata T (2005a) Early-onset macular degeneration with drusen in a cynomolgus monkey (*Macaca fascicularis*) pedigree: exclusion of 13 candidate genes and loci. Invest Ophthalmol Vis Sci 46:683–691

Umeda S, Suzuki MT, Okamoto H, Ono F, Mizota A, Terao K, Yoshikawa Y, Tanaka Y, Iwata T (2005b) Molecular composition of drusen and possible involvement of anti-retinal autoimmunity in two different forms of macular degeneration in cynomolgus monkey (*Macaca fascicularis*). FASEB J 19:1683–1685

Yang Z, Camp NJ, Sun H, Tong Z, Gibbs D, Cameron DJ, Chen H, Zhao Y, Pearson E, Li X, Chien J, Dewan A, Harmon J, Bernstein PS, Shridhar V, Zabriskie NA, Hoh J, Howes K, Zhang K (2006) A variant of the HTRA1 gene increases susceptibility to age-related macular degeneration. Science 314:992–993

Yates JRW, Sepp T, Matharu BK, Khan JC, Thurlby DA, Shahid H, Clayton DG, Hayward C, Morgan J, Wright AF, Armbrecht AM, Dhillon B, Deary IJ, Redmond E, Bird AC, Moore AT (2007) Complement C3 variant and the risk of age-related macular degeneration. N Engl J Med 357:553–561

Yoshida T, Wan AD, Zhang H, Sakamoto R, Okamoto H, Minami M, Obazawa M, Mizota A, Tanaka M, Saito Y, Takagi I, Hoh J, Iwata T (2007) HTRA1 promoter polymorphism predisposes Japanese to AMD. Mol Vis 13:545–548

Acta Ophthalmologica

Letter to the Editor

Stargardt Disease with Preserved Central Vision: identification of a putative novel mutation in ATP-binding cassette transporter gene

Kaoru Fujinami,[1] Masakazu Akahori,[2] Masaki Fukui,[1] Kazushige Tsunoda,[1] Takeshi Iwata,[2] and Yozo Miyake[1,3]

[1]Laboratory of Visual Physiology, National Institute of Sensory Organs, Meguro-ku, Tokyo, Japan
[2]Division of Molecular & Cellular Biology, National Institute of Sensory Organs, National Hospital Organization, Tokyo Medical Center, Meguro-ku, Tokyo, Japan
[3]Aichi Shukutoku University, Aichi, Japan, Nagakute-cho, Aichi-gun, Aichi, Japan

doi: 10.1111/j.1755-3768.2009.01848.x

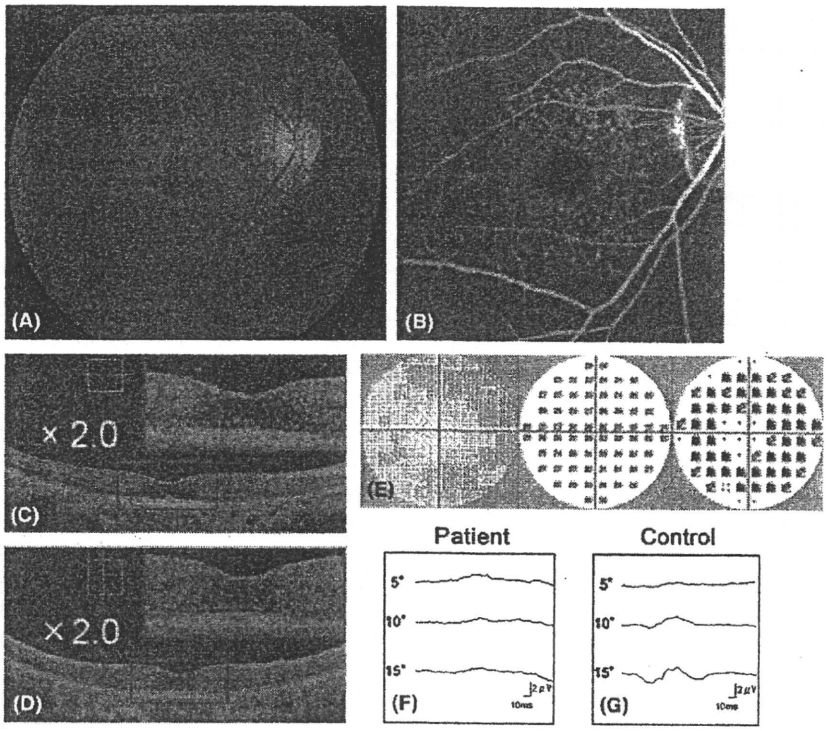

Fig. 1. Fundus photograph (A), fluorescein angiogram (FA) (B), optical coherence tomography (OCT) (C, D), Humphrey static perimetry (E), and focal macular electroretinograms (FMERGs) (F) of an eye of a patient with Stargardt disease. (A) Fundus photograph showing dark brown, well demarcated area in the fovea surrounded by orange-yellow flecks in the macula. (B) FA showing blockage in the foveal area, ring-shaped mottled hyperfluorescence in the macula, and dark choroid. (C, D) OCT images (C; horizontal, D; vertical) showing well-preserved sensory retina and retinal pigment epithelium (RPE) layer in the fovea. In the juxtafoveal region, an atrophy of both sensory retina and RPE can be seen. The enlarged images within the red lines are attached. (E) Humphrey static perimetry showing ring-shaped paracentral relative scotoma (10-2 strategy). (F, G) FMERGs showing normal responses elicited by a 5-degree stimulus spot and severely reduced responses elicited by 10-degree and 15-degree spots, when compared with the age-matched control.

Editor,

Stargardt disease (STGD) has a juvenile to young–adult onset, a rapid decrease of central vision and a progressive bilateral atrophy of the sensory retina and retinal pigment epithelium (RPE) in the macula. Yellow-orange flecks are often detected around the macula, the midretina and or both (Rotenstreich et al. 2003). Mutations in the gene encoding the ATP-binding cassette transporter gene (ABCA4) are responsible for autosomal recessive STGD (Allikmets 1997; Webster et al. 2001). We examined a patient who had the characteristic signs of STGD but had good visual acuity.

A 66-year-old man complained of photophobia and a paracentral scotoma which was present since his teens and had not worsened. None of his family members had similar symptoms. His visual acuity was 20/15 OU, and ophthalmoscopy identified a dark brown, well-demarcated area at the fovea surrounded by RPE atrophy and flecks (Fig. 1A). Fluorescein angiography showed window defects at the flecks and a dark choroid (Fig. 1B). The optical coherence tomographic (OCT) images showed a well-preserved sensory retina and normal thickness RPE at the fovea (Fig. 1C, D). The foveal area was surrounded by atrophic sensory retina and RPE. Static perimetry showed ring-shaped paracentral relative scotoma which surrounded the normal area seeing area of 5° (Fig. 1E). Focal macular electroretinograms (FMERGs) also demonstrated a well-preserved retinal function at the fovea (Fig. 1F). Compared to age-matched controls, the FMERGs had normal responses elicited by a 5-degree stimulus spot and severely reduced responses elicited by 10-degree and 15-degree spots (Fig. 1F, G). Genetic analysis with direct DNA sequencing of amplified products revealed four reported polymorphisms (Allikmets 1997; Briggs et al. 2001; Webster et al. 2001; Fukui et al. 2002) and one novel mutation, Met280Thr, in exon 7 of the ABCA4 gene (Table 1).

Our patient had clinical findings that were pathognomonic of typical STGD, except that the clinical course was stationary and he had 20/15 vision because of well-preserved foveal function. The preserved foveal area was small and well demarcated. Visual acuity, fundus appearance, OCT images, static perimetry and FMERGs supported the well-preserved foveal function. We report our case because the patient had a unique phenotype with a novel putative mutation in the *ABCA4* gene, not yet shown to segregate with the disease.

The well-demarcated dark brown foveal RPE appeared to be hyperpigmented although the thickness measured by OCT was 29 μm which was

Table 1. ABCA4 GENE MUTATION AND Polymorphisms.

Exon	Nucleotide Change	Effect Changes	Het/Hom	References
Mutation				
7	c.839T > C	p.Met280Thr	Het	Present study
Polymorphisms				
10	c.1269C > T	p.His424His	Hom	Webster AR et al.
45	c.6249C > T	p.Ile2083Ile	Het	Allikmets R et al.
46	c.6285T > C	p.Asp2095Asp	Het	Briggs CE et al.
49	c.6764G > T	p.Ser2255Ile	Het	Allikmets R et al.

The translational start codon ATG/methionine is numbered as +1. One novel disease-associated mutation [c.839T > C (p.Met280Thr)] was found. References of previously reported polymorphisms are indicated.
Het, heterozygote; Hom, homozygote.

within normal limits. The findings in our case could indicate that the non-atrophic foveal RPE had an effect in preserving the foveal morphology and function.

The inheritance of STGD is autosomal recessive; however, our patient had four polymorphisms and one heterozygous gene mutation c.839T > C in exon 7 in the *ABCA4* gene. A second mutation was not found, but it may well exist outside of the coding sequence of the *ABCA4* gene. The new mutation in our patient was located outside the known functional domains of ATP-binding or transmembrane site (Lewis et al. 1999), which may explain the mild effect of the missense mutation. We should also consider a modifier gene effect in our patient.

Although the relationship between the new mutation of the *ABCA4* gene and the well-preserved foveal structure is unresolved, the unique phenotype and genotype of our patient may give additional information on the mechanism of photoreceptor degeneration in eyes with STGD.

References

Allikmets R (1997): A photoreceptor cell-specific ATP-binding transporter gene (ABCR) is mutated in recessive Stargardt macular dystrophy. Nat Genet **17**: 122.

Briggs CE, Rucinski D, Rosenfeld PJ, Hirose T, Berson EL & Dryja TP (2001): Mutations in ABCR (ABCA4) in patients with Stargardt macular degeneration or cone-rod degeneration. Invest Ophthalmol Vis Sci **42**: 2229–2236.

Fukui T, Yamamoto S, Nakano K et al. (2002): ABCA4 gene mutations in Japanese patients with Stargardt disease and retinitis pigmentosa. Invest Ophthalmol Vis Sci **43**: 2819–2824.

Lewis RA, Shroyer NF, Singh N et al. (1999): Genotype/Phenotype analysis of a photoreceptor-specific ATP-binding cassette transporter gene, ABCR, in Stargardt disease. Am J Hum Genet **64**: 422–434.

Rotenstreich Y, Fishman GA & Anderson RJ (2003): Visual acuity loss and clinical observations in a large series of patients with Stargardt disease. Ophthalmology **110**: 1151–1158.

Webster AR, Heon E, Lotery AJ et al. (2001): An analysis of allelic variation in the ABCA4 gene. Invest Ophthalmol Vis Sci **42**: 1179–1189.

Correspondence:
Kazushige Tsunoda, MD
Laboratory of Visual Physiology
National Institute of Sensory Organs
2-5-1 Higashigaoka
Meguro-ku
Tokyo 152-8902
Japan
Tel: + 81 3 3411 0111 ext. 6615
Fax: + 81 3 3412 9811
Email: tsunodakazushige@kankakuki.go.jp

Exp. Anim. 59(2), 171–182, 2010

—Original—

Comparative Proteomic Analyses of Macular and Peripheral Retina of Cynomolgus Monkeys (*Macaca fascicularis*)

Haru OKAMOTO[1, 2], Shinsuke UMEDA[1], Takehiro NOZAWA[3], Michihiro T. SUZUKI[4], Yasuhiro YOSHIKAWA[5], Etsuko T. MATSUURA[6], and Takeshi IWATA[1]

[1]*Division of Molecular & Cellular Biology, National Institute of Sensory Organs, National Hospital Organization Tokyo Medical Center, 2–5–1 Higashigaoka, Meguro-ku, Tokyo 152-8902, Japan,* [2]*Department of Advanced Biosciences, Ochanomizu University, 2–1–1 Otsuka, Bunkyo-ku, Tokyo 112-8610, Japan,* [3]*Analytical Instrument Division, AMR Inc., 2–13–18 Nakane, Meguro-ku, Tokyo 152-0031, Japan,* [4]*The Corporation for Production and Research of Laboratory Primates, 1–1 Hachimandai, Tsukuba-shi, Ibaraki 305-0843, Japan,* [5]*Department of Biomedical Science, Graduate School of Agricultural and Life Sciences, The University of Tokyo, 1–1–1 Yayoi, Bunkyo-ku, Tokyo 113-8657, Japan, and* [6]*The Natural/Applied Sciences Division, Ochanomizu University, 2–1–1 Otsuka, Bunkyo-ku, Tokyo 112-8610, Japan*

Abstract: The central region of the primate retina is called the macula. The fovea is located at the center of the macula, where the photoreceptors are concentrated to create a neural network adapted for high visual acuity. Damage to the fovea, e.g., by macular dystrophies and age-related macular degeneration, can reduce central visual acuity. The molecular mechanisms leading to these diseases are most likely dependent on the proteins in the macula which differ from those in the peripheral retina in expression level. To investigate whether the distribution of proteins in the macula is different from the peripheral retina, proteomic analyses of tissues from these two regions of cynomolgus monkeys were compared. Two-dimensional gel electrophoresis and mass spectrometry identified 26 proteins that were present only in the macular gel spots. The expression levels of five proteins, cone photoreceptor specific arrestin-C, γ-synuclein, epidermal fatty acid binding protein, tropomyosin 1α chain, and heterogeneous nuclear ribonucleoproteins A2/B1, were significantly higher in the macula than in the peripheral retina. Immunostaining of macula sections by antibodies to each identified protein revealed unique localization in the retina, retinal pigment epithelial cells and the choroidal layer. Some of these proteins were located in cells with higher densities in the macula. We suggest that it will be important to study these proteins to determine their contribution to the pathogenesis and progression of macula diseases.

Key words: 2D-gel electrophoresis, macula, mass spectrometry, retina

(Received 16 September 2009 / Accepted 13 November 2009)

Address corresponding: T. Iwata, Division of Molecular & Cellular Biology, National Institute of Sensory Organs, National Hospital Organization Tokyo Medical Center, 2–5–1 Higashigaoka, Meguro-ku, Tokyo 152-8902, Japan

Introduction

The macula is an oval-shaped, highly pigmented spot near the central region of the primate retina. It is approximately 2.0 mm in diameter in humans [31] and 1.0 mm in macaque monkeys [36–38]. The fovea is located at the center of macula where the retinal thickness is reduced to approximately 0.1 mm and consists of only the retinal pigment epithelium (RPE), photoreceptor layer, external limiting membrane, outer nuclear layer, outer plexiform layer, and inner limiting membrane [30]. The cone density in the foveal pit is the highest in the retina, and rods, retinal ganglion cells (RGCs), and blood vessels are not present. These cones are connected to large numbers of RGCs, which are highly dense at the parafovea [31]. The cone-dense fovea mediates high-acuity central vision, and any damage to the macula can lead to severely depressed central visual acuity as observed in patients with macular dystrophies and age-related macular degeneration (AMD).

Because of the unique cellular organization of the macula, investigators have performed comprehensive gene expression studies of the macula and peripheral retina using DNA microarray analysis or Serial Analysis of Gene Expression (SAGE). Sharon *et al.* used SAGE to show that several genes are preferentially expressed in the human macula and RPE. Most of these genes are associated with the function of the RGCs, and were presumably detected because of the high density of RGCs in the macula [35]. Bowes Rickman *et al.* also performed SAGE on human retinas and isolated RPE cells and identified genes that are abundantly expressed in cones, RGCs, and RPE cells [3]. Ishibashi *et al.* performed 4 K DNA microarray analysis on RPE cells from the macula and reported five differentially expressed genes which were confirmed by real-time PCR [18]. Recently, Radeke *et al.* [32] and van Soest *et al.* [48] used 22 K DNA microarray analyses and identified a number of genes that were differentially expressed in the macula and peripheral retina. In each study, five of these genes were found to be highly expressed in RPE cells in the macula. van Soest *et al.* showed by immunohistochemistry that the WAP four-disulfide core domain 1, one of the highly expressed proteins, is present in the RPE cells in the macula. However, the expression level of the mRNAs does not always correlate with the expression levels of the proteins.

Recent technical advances in proteomics allow the direct determination of the protein profile of body fluids and tissue homogenates. Proteomic analyses of the retina were first performed by Nishizawa *et al.* [28], and several groups have catalogued the retinal proteins using single or two-dimensional (2D) gel electrophoresis followed by mass spectrometry (MS) analysis [1, 5, 50]. Ethen *et al.* examined cadaver eyes with AMD by proteomic analyses and reported that the expression of proteins changed with the progression of AMD, and the changes in the macula were different from those in the peripheral retina [10]. These findings indicate that the macular region of the retina is different from the peripheral retina not only in its morphology but also in its protein content.

Proteomic studies of the macula are difficult to perform because of the lack of fresh human eyes, and small sample size of the macula. To overcome these problems, we selected non-human primate eyes of the cynomolgus monkey (*Macaca fascicularis*). The retina and visual system of macaque monkeys are quite similar to those of humans [14, 29], and monkeys with characteristics of macular diseases have been reported by many investigators [9, 16, 19, 25, 39, 40] as well as our previous studies [26, 27, 44–47]. Thus, the purpose of this study was to identify proteins present at high levels in the macula to better understand the biology of this unique tissue. To accomplish this task, we performed proteomic analyses on retinal tissues obtained from the macular region and the periphery for comparison.

Materials and Methods

Preparation of cynomolgus monkey eyes

All experiments on monkeys were approved by the Animal Ethics Committee of the Tsukuba Primate Research Center (TPRC) and were conducted in accordance with The Association for Research in Vision and Ophthalmology Statement for the Use of Animals in Ophthalmic and Vision Research. Eight eyes from eight normal female cynomolgus monkeys (*Macaca fascicularis*) whose ages ranged between 13 to 19 years were studied. Eyes were removed approximately one hour

after death and treated with RNAlater (Applied Biosystems, Tokyo, Japan). Other tissues from these animals were used by other research groups at the TPRC. Three-millimeter-diameter pieces of macular and peripheral retina containing neural retina, RPE and choroidal layer were punched out and frozen until use. The proteins extracted from the tissues of eight eyes were pooled for the analyses.

Protein extraction and 2D-gel electrophoresis

The proteins from the macula and peripheral retina were extracted after homogenization and sonication in sample buffer [7 M urea, 2 M thiourea, 4% CHAPS, 50 mM DTT, 40 mM Tris, 0.2% Bio-Lyte 3/10 (Bio-Rad, Hercules, CA, USA)]. After centrifugation for 15 min × 3 at 14,000 rpm (20,800 × *g*), the supernatant was collected. The lysate was precipitated using Ready Prep 2D cleanup kit (Bio-Rad) and redissolved in sample buffer. The protein concentration was determined with the RC-DC protein assay kit (Bio-Rad) according to the manufacturer's instruction. Protein samples (300 μg) were separated by isoelectric focusing (IEF) using 17-cm immobilized pH gradient (IPG) strips. After 12 to 16 h of rehydration at 20°C, the IEF sample was used for the first dimension with an initial voltage of 250 V for 15 min and then increased to 10,000 V for 3 h and held until 60,000 V-h was reached. Immediately after the IEF, the IPG strips were stored at –20°C until the equilibration step was carried out. The IPG strips were equilibrated for 20 min in buffer containing 6 M urea, 2% SDS, 0.375 M Tris (pH 8.8), and 20% glycerol under reduced conditions with 2% DTT, followed by another incubation for 10 min in the same buffer under alkylating conditions with 2.5% iodoacetamide. The equilibrated IPG strips were electrophoresed for the second dimension using 12% acrylamide gels. Two dimensional gel electrophoresis was performed at four different pH ranges, viz., pH 3–10, 4–7, 5–8, and 7–10. After the 2D gel electrophoresis, the proteins were stained with SYPRO Ruby (Bio-Rad). The images for the macula and peripheral retina were compared with ImageMaster 2D Platinum ver.5.0 (GE Healthcare Bio-Sciences, Piscataway, NJ, USA) followed by visual inspection. The gel spots numbered in Fig. 1 were excised. Two dimensional gels of peripheral retina were stained with Bio-safe Coomassie (Bio-Rad). Then, 46 spots from the Coomassie-stained gel were excised (Fig. 1, Peripheral Coomassie).

In gel digestion and LC-MS/MS analyses

Each gel piece was cut into approximately one cubic millimeter and washed twice with 50 mM ammonium bicarbonate/50% acetonitrile. After destaining, the gel pieces were rinsed with distilled water, and incubated with acetonitrile for 20 min. The supernatant was discarded and the gel pieces were completely dried before incubation with 10 mM DTT in 100 mM ammonium bicarbonate for 45 min at 56°C. The supernatant was discarded and the pieces were incubated in the dark with 55 mM iodoacetamide in 100 mM ammonium bicarbonate (30 min, at room temperature). The supernatant was discarded, and the gels were washed three times. Finally, the gel pieces were completely dried before tryptic digestion in sequencing grade trypsin solution (12.5 ng/μl; Promega, Madison, WI, USA) in 50 mM ammonium bicarbonate. The digestion was performed at 37°C overnight, and the extraction step was performed once with 25 mM ammonium bicarbonate, twice with 5% formic acid, and finally with distilled water. The extracted peptides were pooled and dried. After re-suspending in 40 μl of aqueous 0.01% trifluoroacetic acid/2% acetonitrile, the samples were analyzed by LC (liquid chromatography)-MS/MS. LC-MS/MS was performed with a combined Paradigm MS4 (Michrom BioResources, Auburn, CA, USA) and an ESI mass spectrometer (LCQ Deca XP plus or Finnigan LTQ, Thermo Fisher Scientific, Yokohama, Japan; assembled by AMR Inc., Tokyo, Japan). For the LCQ analysis, sample peptides were separated in nano column (AMR Inc.) with solvent A (2% acetonitrile/0.1% formic acid) and B (90% acetonitrile/0.1% formic acid) at flow rate of 0.6 μl/min, gradient of 5 to 95% solvent B over 40 min. For the LTQ analysis, peptides were separated on Magic C18 (Michrom BioResources) with solvent A and B, a flow rate 1.5 μl/min, gradient of 5 to 95% solvent B over 30 min. The identification of the proteins from the MS/MS spectra was performed using protein identification software (Bioworks ver.3.1, Thermo Fisher Scientific) and UniProtKB/Swiss-Prot database (Release 48.8) which was preliminarily extracted by the species "human" (13,361 entries). Peak list generation and database searches were performed with the following

parameters: mass tolerance for precursor ions, 2.5 amu; mass tolerance for fragment ions, 0.00 amu; enzymatic cleavage position, after lysine or arginine; number of missed cleavage sites permitted, 2; fixed modification, carbamide-methylation (+57.02 Da) for cysteine; variable modification, oxidation (+16 Da) for methionine. The peptide sequences were filtered by delta Cn score and peptide Cross Correlation (XC) score. The threshold level of delta Cn scores was >0.1 for peptide sequences from both measurement devices. The threshold levels of XC scores for each charge (+1/+2/+3) were >1.5/2.0/3.7 for LCQ and >1.9/2.2/3.7 for LTQ. Then, the correlations between the observed in gel images and the theoretical molecular weight and pI were considered. When peptides matched multiple members of the protein family, the protein which had the most number of peptides that matched the amino acid sequence was selected. In case of equal numbers, both proteins were listed.

Western blotting and immunohistochemical analysis of macula

Five to fifteen micrograms of macula or peripheral retinal homogenates were diluted in a double volume of SDS buffer and separated by 1D-PAGE followed by transfer to PVDF (polyvinylidene difluoride) membrane. Membranes were blocked with blocking solution (Blocking Solution Concentrate, KPL, Gaithersburg, MD, USA), skim milk, or BSA dissolved in PBS and probed with one of the following primary antibodies (Abs): chicken Ab to human arrestin-C (GenWay Biotech, San Diego, CA, USA), rabbit Ab to human synuclein gamma (Novus Biologicals, Littleton, CO, USA), rat Ab to human epidermal fatty acid binding protein (E-FABP) (R&D Systems, Minneapolis, MN, USA), rabbit Ab to tropomyosin Br-1, Br-3 (CHEMICON International, Temecula, CA, USA), mouse Ab to chicken tropomyosin TM311 (Abcam, Cambridge, UK), and goat Ab to human heterogeneous nuclear ribonucleoproteins (hnRNPs) A2/B1 (Santa Cruz Biotechnology, Santa Cruz, CA, USA). The specific signals were detected with one of the following secondary antibodies: horseradish peroxidase (HRP)-conjugated goat Ab to mouse IgG (Jackson ImmunoResearch Laboratories, West Grove, PA, USA), HRP-conjugated goat Ab to rabbit IgG (Pierce, Rockford, IL, USA), HRP-conjugated rabbit Ab to chicken/turkey IgG (Zymed Laboratories, South San Francisco, CA, USA), HRP-conjugated donkey Ab to goat IgG (Jackson ImmunoResearch Laboratories), HRP-conjugated goat Ab to rat IgG (Zymed Laboratories). The signals were made visible by chemiluminescence reactions and examined with a chemiluminescence imager (Lumi-Imager F1; Roche Diagnostics, Tokyo, Japan). An enucleated eye from a normal female cynomolgus monkey (age 13 years) was fixed in 10% neutralized and buffered formaldehyde solution at 4°C overnight and then dehydrated. The specimens were embedded in paraffin and serially sectioned at 4 μm thickness. The specimens were treated for antigen retrieval by autoclaving in Target Retrieval Solution (Dako, Carpinteria, CA, USA) for 20 min at 121°C. The sections were then blocked with Dako Protein Block (Dako) or skim milk or BSA in PBS. The primary antibodies were the same as used for the western blotting, and rabbit Ab to human platelet/endothelial cell adhesion molecule (PECAM1) (Proteintech Grroup, Chicago, IL, USA). For signal detection after rinsing off the primary antibodies, the sections were incubated with one of following secondary antibodies: Alexa 488-conjugated goat Ab to anti-mouse IgG, Alexa 568-conjugated goat Ab to anti-mouse IgG, Alexa 488-conjugated goat Ab to anti-rabbit IgG, Alexa 568-conjugated goat Ab to anti-rabbit IgG, Alexa 488-conjugated donkey Ab to anti-goat IgG, Alexa 568-conjugated goat Ab to anti-chicken IgG, and Alexa 488-conjugated goat Ab to anti-rat IgG (all secondary antibodies from Invitrogen, Tokyo, Japan). After rinsing off the antibodies, the sections were examined by confocal laser scanning microscope (Radiance 2100, Bio-Rad). The cell nuclei were stained with DAPI (4',6-diamino-2-phenylindole). To determine the location of the signals, one of the sections was stained with hematoxylin and eosin.

Results

Identification of macula enriched proteins

Approximately 700 spots were detected in the macular and peripheral retinal tissues in the 2D gel stained with SYPRO Ruby (pH range 3–10; Fig. 1A). Sixty percent of these spots were found in both samples. Butt *et al.* have described the difficulties of IEF separation by RNAlater contaminations [4]. Our samples were de-

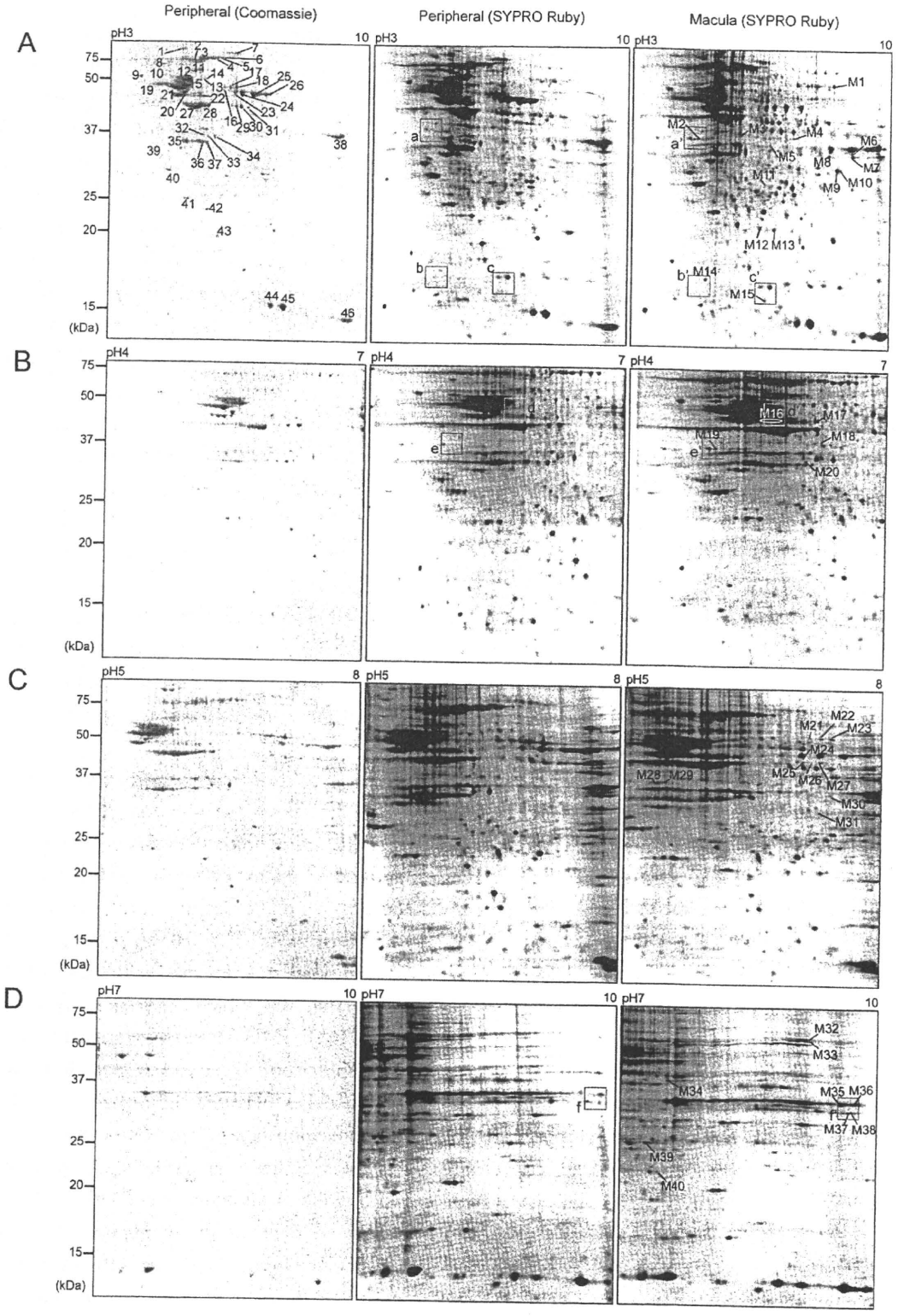

Fig. 1. Separation of monkey retina proteins on 2D gels. Proteins extracted from the peripheral retina and macula (300 μg each) were isoelectric focused at four different pH ranges; pH 3–10 (A), 4–7 (B), 5–8 (C), 7–10 (D). Then the IPG strips were separated on 12% SDS-page gels and stained by SYPRO Ruby. Forty spots marked by spot IDs were unique to the macula gel images and identified by LC-MS/MS. Boxed areas (a–f, Peripheral-SYPRO Ruby; a'–f', Macula-SYPRO Ruby) correspond to the enlarged images in Fig. 2. Two dimensional gels of peripheral retina were also stained by Bio-safe Coomassie. Forty-six spots marked by spot number were identified by LC-MS/MS.